Combust. Sci. and Tech., 180: 699–712, 2008

ISSN: 0010-2202 print/1563-521X online
DOI: 10.1080/00102200701845524

PUFFING FREQUENCY AND SOOT EXTINCTION CORRELATION IN JP-8 AND HEPTANE POOL FIRES

Tara L. Henriksen[1], Terry A. Ring[1], Eric G. Eddings[1], and G. J. Nathan[2]

[1]*Department of Chemical Engineering, University of Utah, Salt Lake City, UT*

[2]*School of Mechanical Engineering, University of Adelaide, S.A., Australia*

A new approach for characterizing puffing frequency was established by performing total extinction measurements on pool fires of JP-8 (Jet Propulsion Fuel 8) and heptane using a multiple beam extinction experiment. A maximum entropy method (MEM) was applied to extract a characteristic extinction frequency that was found to correlate well with puffing frequency. The measured extinction frequency for both flames was found to have some variation with height, though this is small. The amplitude of the frequency of the measured oscillations was found to be higher for JP-8 than for heptane, and became constant one diameter above the fuel pan for both flames. The variance of total extinction in the JP-8 and heptane pool fires was approximately 20% and 17%, respectively. Correlation statistics between the various extinguished beams reveal an increase in axi-symmetry of the instantaneous oscillations with height above the pool.

Keywords: Pool fires; Puffing frequency; Soot

INTRODUCTION

Many accidental fires result from the leak or spill of liquid fuel that is subsequently exposed to an ignition source. Analysis of these so-called pool fires is complex due to buoyancy-driven turbulence, variable entrainment of surrounding air, and the coupling between the flame radiation and the evaporating fuel. The study of Bouhafid et al. (1988) into the nature of the flame structure in pool fires revealed three distinct regions; the base region, the necking or "intermittent" region, and the plume region at the top of the flame. The frequency of the large-scale oscillations

Received 15 November 2006; accepted 9 November 2007

This work was sponsored by the Center for the Simulation of Accidental Fires and Explosions at the University of Utah, which was funded by the U.S. Department of Energy under Contract No. LLL B341493, with matching funds provided by the University of Utah Research Fund. Equipment was provided by the Australian Research Council. The authors would like to gratefully acknowledge the support of Zeyad Alwahabi, Nader Qamar and Dr. Keith King at the University of Adelaide; Jennifer Spinti, Phil Smith and Dana Overacker at the University of Utah.

Address correspondence to Tara L. Henriksen, Department of Chemical Engineering, University of Utah, Salt Lake City, UT 84112, USA. E-mail: thenriks@eng.utah.edu

controlling the rate of air entrainment into the flame, and therefore combustion volume, is termed the "puffing frequency" as noted by Weckman (1988).

The most popular technique employed empirically to study the characteristic puffing frequency of a flame is flow visualization (Hamins et al., 1992; Malalaskera et al., 1996; Sato et al., 2000; Eddings et al., 2005). This approach involves taking high speed pictures of the flame and assessing the downstream propagation of the large scale structures. Other methods of puffing frequency characterization include calculating power spectral densities of temperature obtained via thermocouple measurements as done by Weckman (1988), the use of thermal imaging (Malalaskera, 1996), or the measurement of velocity via laser doppler anemometry (Weckman, 1988).

Experimental results (Hamins et al., 1992; Zukoski et al., 1984) have verified that puffing frequency varies as the inverse square root of the burner diameter ($f = 1.5D^{-1/2}$). Most of the measurements to date that quantify a puffing frequency based on methods other than high speed photography, employ intrusive and time-consuming methods. Extinction measurements are commonly carried out for use as a calibration technique for advanced optical methods, and thus many investigators may find it more convenient than the approaches listed above for puffing frequency determinations.

The characteristic puffing frequency can be used as a validation metric for turbulence models that govern the fluid dynamics of a buoyancy-dominated combustion process. One study by Puri (1993) performed a boundary layer analysis of a horizontally situated reacting surface using pulsation frequency. He concluded that it is possible to use a parabolic solution rather than an elliptic one to solve the boundary layer problem, if it is assumed that instabilities grow in amplitude downstream in the flame with an unchanging frequency. However, the validity of this assumption remains uncertain. It's also of interest to determine whether more soot is formed within the puffs or in the necking region between them which would provide insight into the mechanism of soot formation and emission in these kinds of flames. The present paper seeks to address these issues.

The first aim of this work is to demonstrate the efficacy of the use of a time-series of laser extinction data to determine the puffing frequency in pool fires. Our second aim is to provide new physical insight into pool fire behavior through interpretation of the relationship between extinction measurements and puffing frequency.

EXPERIMENTAL SETUP

Pool Fire Pan Design

The pool fire pan was built at the University of Utah (Figure 1). The 76 mm high pan has a 165 mm OD. Cooling water was run through a 13 mm shell surrounding the pool cavity. Fuel entered through a 6 mm opening in the bottom of the pan and passed through a fuel disperser. Thermocouples, located at radial distances of 25 mm and 51 mm, corresponding to heights of 13 mm and 25 mm from the bottom of the pan, reported the temperature of the fuel within the pan to a data acquisition system. A separate reservoir pan, located outside of the fire enclosure, was connected hydrostatically to the burning fuel pan. Fuel level was maintained in the reservoir pan by an ultrasonic level sensor. A PID control program triggered a pump, which replenished fuel to the reservoir pan.

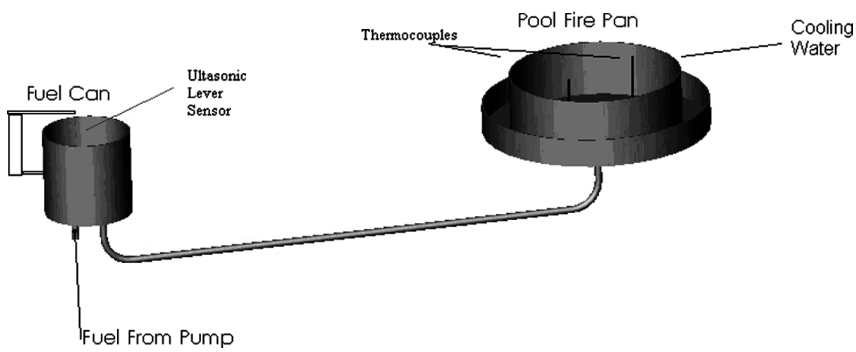

Figure 1 Pool fire pan system.

Cooling water in the fire pan shell was kept at a constant flow rate of 128 ml/min, corresponding to an average exiting water temperature of 76°C, as measured by a thermocouple in the exiting water stream. Fuel level in the pan was maintained at 32 mm $\pm$5 mm. This was effective in controlling the fuel temperature to within $\pm$3.8°C (JP-8) and $\pm$2.6°C (Heptane). As puffing frequency depends on buoyancy, which further depends on flame temperature (and thus fuel type and radiant cooling), flame height (and hence on pan diameter), and on mixing it is desirable to keep these parameters the same.

However, it is not necessary to keep them all identical, since the role of all of dependent variables are reasonably well described by a relation given in Hamins et al. (1992). For this reason we have chosen to keep the pan diameter constant, which resulted in the flame heights being within 7% of each other (0.58 ± 0.01 m and 0.54 ± 0.01 m), and to keep the heat release approximately the same. The average volumetric fuel flow rates for JP-8 and heptane were similar (11.8 cm^3/min and 14.6 cm^3/min), as the same size pan was used in both experiments. The volumetric flow rates of fuel were determined by the need to keep the liquid fuel heights constant for each flame. This corresponds to a heat release rate for the two flames of 0.11 and 0.074 kW, respectively.

Extinction measurements were recorded when the flame reached steady state, as determined by stabilization of the fuel feed rate to the pool fire, as well as the temperatures of cooling water and the unburned fuel. Extinction measurements were performed at five heights in the flame. Measurements were spaced 102 mm apart, and began 2–3 mm above the base of the pan. The distance from the pan base to the hood was 1016 mm, and the hood volumetric flow rate was maintained at a standard condition of 0.69 m^3/s, which was just adequate to withdraw the soot laden plume.

Multiple Beam Extinction Setup

Extinction measurements were conducted using a continuous wave 532 nm laser diode (Model E14034 Electus), operating at 10 mW, in the Turbulence, Energy and Combustion (TEC) lab at the University of Adelaide. A laser beam with a

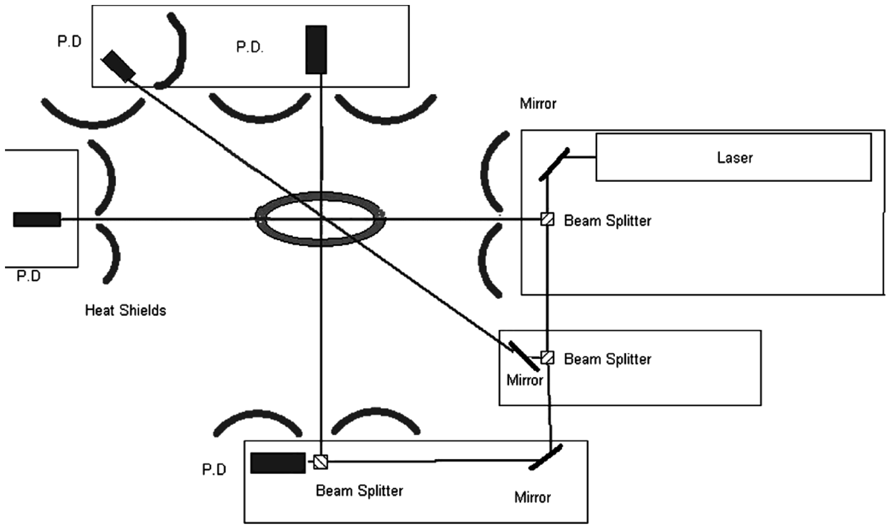

Figure 2 Schematic design of the multiple beam extinction set-up. P.D. = Photodetector.

diameter of 0.5 mm (unfocused) passed through a series of three 50/50 beam splitters (Figure 2). The beams were aligned to cross on the axis of the burner, and were oriented at angles of 0°, 45° and 90° to each other. A fourth beam provided a reference to correct for possible variations in the temporal laser power intensity. Radiative interference was minimized by the use of filters and apertures placed in front of each of the four photodetectors, yielding a maximum signal to noise ratio of 2126:14.

The point-by-point ratio of the attenuated beam to the incident beam yields the attenuation. Three extinction beams were used to determine the axisymmetry of the flame and extinction results are reported as an average of these three beams at each height. The puffing frequency can then be determined independently from any one of the three extinguished beams. The sample size was 200,000 points, which corresponded to approximately 8 minutes of fire time, and the data were recorded at 400 Hz, which is two orders of magnitude faster than the predicted puffing frequency of $\sim$3Hz. Density fluctuations in our turbulent flame resulted in beam steering of approximately 1°, which resulted in approximately ± 2 mm deflection in any direction at the detector. However, our sensor had a diameter of 10 mm so that all of the laser energy was collected by the sensor independent of this effect.

THEORETICAL CONSIDERATIONS

FFT and MEM Analysis

Traditionally, power spectral densities (PSD) are calculated to determine the characteristic frequencies of a signal (Becker, 1976). A Fourier transform PSD maps a function existing in the time domain (signal input) into another function (signal output) existing in the frequency domain. Given a set of time series data points acquired over a given time period $x(t)$, the forward Fourier transform to the frequency domain is given by

$$X(\omega) = \frac{1}{\sqrt{2\pi}} \int_{-\infty}^{\infty} x(t) e^{-i\omega t} dt \tag{1}$$

where ω is the frequency, and t is time.

A fast Fourier transform (FFT) algorithm was utilized to identify peaks in extinction PSDs. The peak with a low frequency and a high power corresponds to the puffing frequency. However, due to the turbulent nature of the flame, the FFTs were far too noisy to confidently identify a single low frequency peak that would characterize large-scale puffing behavior (Figure 3), and thus an alternative approach was sought.

The maximum entropy method (MEM) is built upon the statistical theory that, "of all the possible solutions, we should use the one with the maximum entropy" (Wu, 1997). In thermodynamics and statistical mechanics, entropy is a measure of the degree of disorder of a system. Its equivalent meaning in modern information theory is the uncertainty of an information source, and it is this meaning of entropy that is employed here. Its advantage in seeking the puffing frequency in pool fires is its capacity to reduce high frequency noise and resolve low frequency information.

By maximizing the entropy (S) in Eq. (2), an expression for maximum entropy is obtained in terms of the power spectral density x(ω) of the signal, where the integral is taken over the entire frequency band, and ω is the frequency.

$$S = \int \log x(\omega) d\omega \tag{2}$$

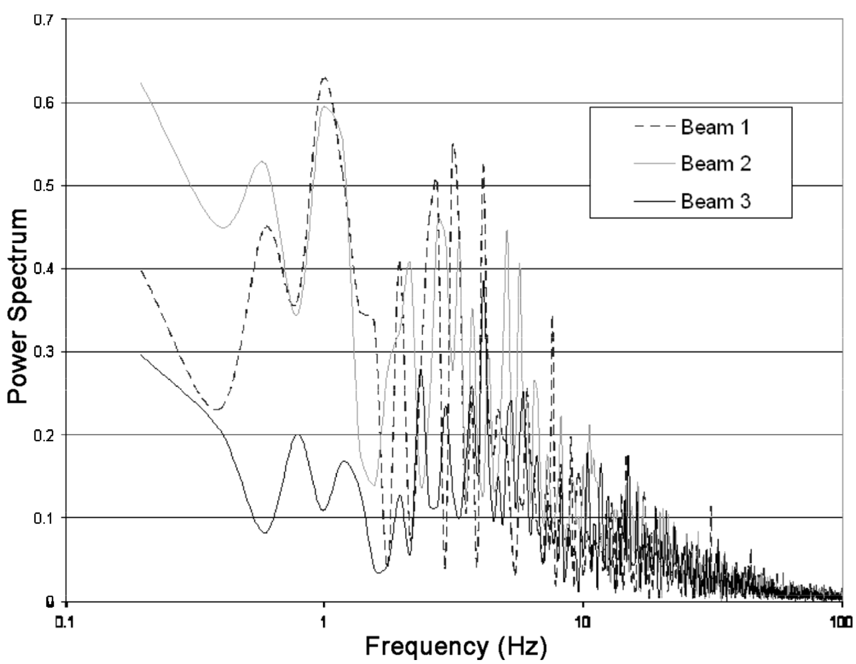

Figure 3 Sample FFT calculated from three extinguished beams through one height for JP-8. Noisy FFT makes it difficult to confidently determine a single peak.

An autoregressive moving average digital filter is built to remove the details from the spectrum of the signal and leave only white noise. The inverse of this filter then yields the power spectrum of the original signal, whose explicit solution is given in Eq. (3),

$$x(\omega) = \frac{p_M}{\left|\sum_{k=0}^{M} a_k \exp(-2\pi i \omega k)\right|^2} \tag{3}$$

where p_M is the power of prediction error, $i = \sqrt{-1}$, a_k are the coefficients of the prediction error filter and M is the order of the filter (Wu, 1997). The estimation of coefficients from the moving average filter were used to calculate an MEM spectrum via the Burg method (Burg, 1967).

RESULTS AND DISCUSSION

Extinction

The probability distributions of the ratio of total incident to extinguished beams averaged over each height are shown in Figure 4. The distribution of local extinction results obtained in the pool fire of JP-8 is skewed towards the low side of the mean. In contrast, results for heptane show the opposite trend, in which they

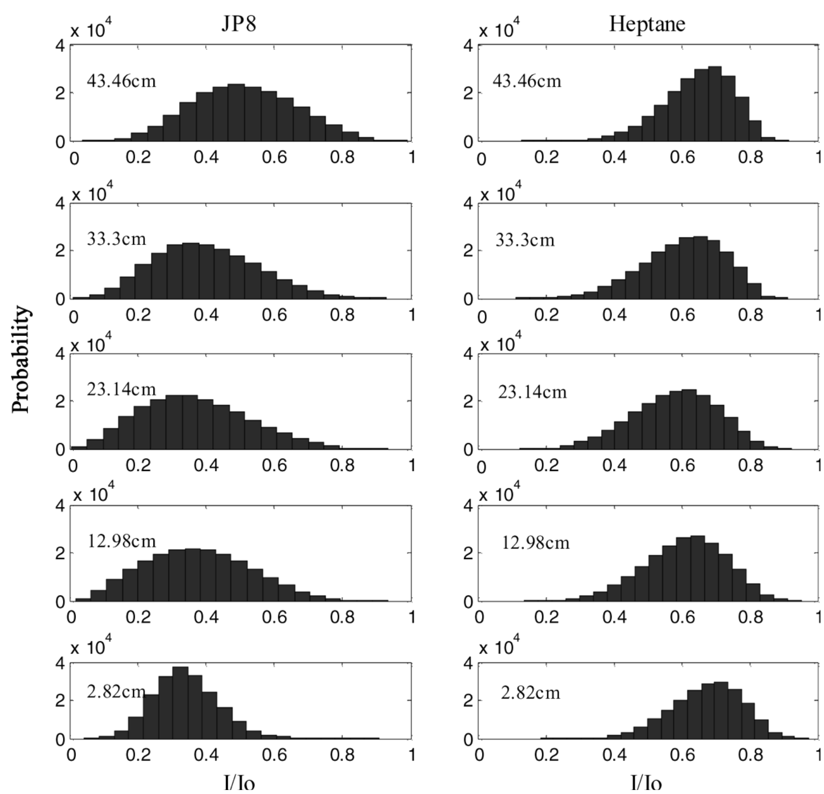

Figure 4 Histograms representing the distribution of the ratio of I/Io in JP-8 (left) and Heptane (right) at 5 heights in the flame. Results taken from 200,000 data points and represent an average of 3 beams.

Table 1 Statistical values of total transmission (I/Io) for JP-8 and Heptane at each height in the flame

	JP-8				Heptane			
Height (mm)	Mean	Std. dev	Skewness	Kurtosis	Mean	Std. dev	Skewness	Kurtosis
434.6	0.5128	0.1997	0.1030	2.5191	0.6490	0.1492	0.5923	3.2349
333	0.4010	0.1980	0.2832	2.6360	0.6059	0.1751	0.4397	2.8150
231.4	0.3679	0.2122	0.3227	2.6292	0.5789	0.1839	0.2843	2.6617
129.8	0.3770	0.2222	0.2300	2.5572	0.6101	0.1750	0.2827	2.7533
28.2	0.3415	0.1650	0.3503	3.2042	0.6729	0.1650	0.3656	2.8861
Avg.	0.4000	0.1995	0.2579	2.7091	0.6234	0.1696	0.3929	2.8702

Results taken from sample sizes of 2,00,000 data points.

are skewed toward the high, or lesser attenuated side of the mean. Third moment calculations of the extinction data determine the skewness. Skewness results show both JP-8 and heptane are positively skewed (Table 1).

The less positively skewed distribution functions of JP-8 point to the observation that the puffs, as measured by extinction are larger, and the necking region connecting them is shorter than for heptane. This is most likely due to the presence of significant quantities of soot in the JP-8 flame being outside the visible flame boundary, in contrast to that in the heptane flame. Evidence for the extra soot in the JP-8 flame can be seen in Figure 5, where cooler, unburned soot can be seen outside the luminous region of the puff in Region 3.

Kurtosis, the fourth moment, measures the propensity of a data set to have outliers, and a normal distribution has a kurtosis of 3.0. Kurtosis values greater than 3.0 indicate a more peaked distribution than that of a normal distribution; values less than 3.0 indicate a flatter distribution. Values of kurtosis for JP-8 decrease as a

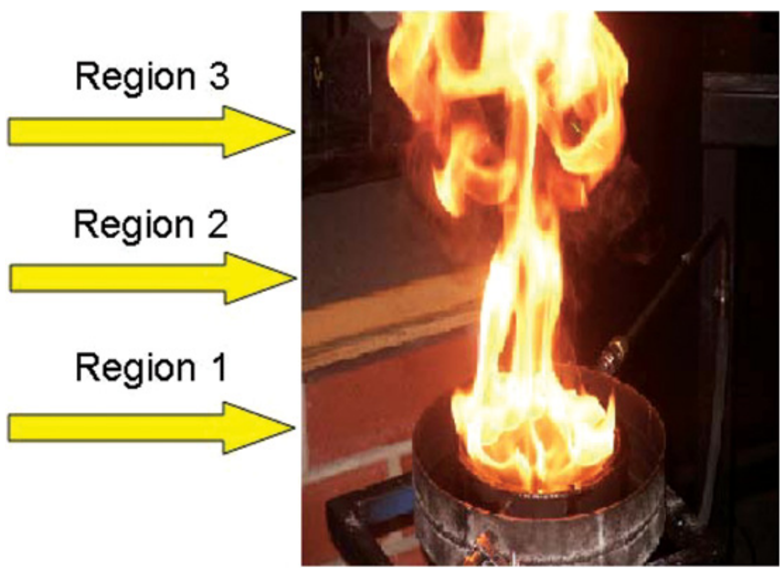

Figure 5 Depiction of three flame regions: Region 1 is the flame base, Region 2 is the necking or intermittent region and Region 3 is the plume region.

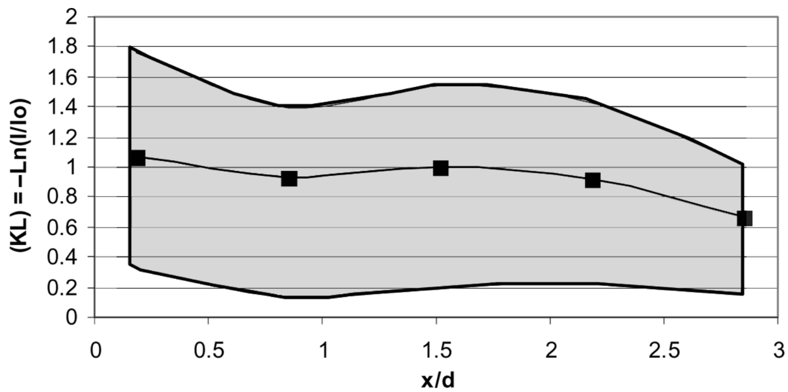

Figure 6 Average values for the natural logarithm of modified extinction (KL) for JP-8 at each height, obtained from all extinguished beams. Shaded area indicates the standard deviation of the probability distributions propagated through the natural log from the raw data set.

function of height (tendency for outliers becomes greater closer to the pool); whereas for heptane, outliers decrease moving towards the pool, and then increase again at a height one diameter above the pool surface. The mean and standard deviation of total extinction for the distributions of JP-8 and heptane, respectively, are 40% ± 20% and 62% ± 17%.

Extinction coefficient values were calculated according to Eq. (4)

$$(KL) = -\ln\left(\frac{I}{I_o}\right) \tag{4}$$

giving the values in Figures 6 and 7 for JP-8 and heptane, respectively. The shaded area shown reflects the standard deviation in the probability distributions shown in Figure 4. A modified extinction coefficient (KL) was computed instead of the traditional extinction coefficient (K) as given by Kohse-Hoinghaus (2002), due to the error associated with choosing an accurate value for path length (L). In heavily

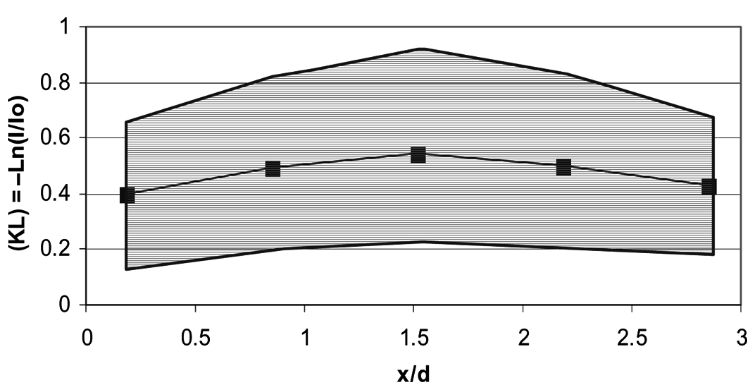

Figure 7 Average values for the natural logarithm of modified extinction (KL) for heptane at each height, obtained from all extinguished beams. Shaded area indicates the standard deviation of the probability distribution propagated through the natural log from the raw data set.

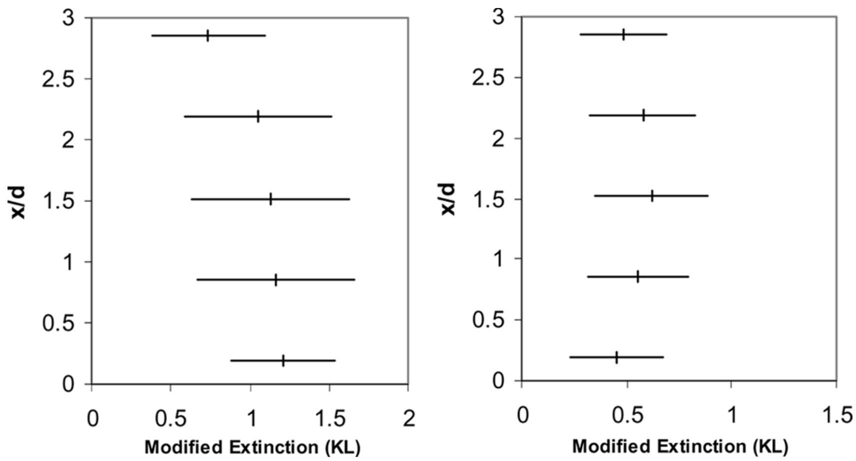

Figure 8 Modified extinction coefficients as a function of height above the fuel surface. Crosses indicate time averaged values, while bars indicate the range of ± 1 standard deviation of the measured PDF about the mean.

sooting flames like JP-8, where non-radiating soot obstructing the optical path length can lay outside the flame envelope, choosing L based on the flame envelope is certainly incorrect, and estimating the extent of non-radiating soot is difficult.

Nonetheless, some observations can be made about trends in the modified extinction coefficient (KL). The average value for the modified extinction coefficient shows an decreasing trend with height for JP-8 (Figure 6); whereas, that for heptane (Figure 7) shows a maximum at a height approximately 1.5 burner diameters above the pool. A constantly decreasing trend in the average modified extinction coefficient (KL) physically means that, for JP-8, more soot is found with decreasing height in the flame. That is, the rate of soot production exceeds that of oxidation throughout the flame. This is consistent with the observation of considerable emission of soot from the flame. For heptane, the average modified coefficient increases up to 1.5 diameters above the pool and then decreases. This is consistent with the observation of a lower emission of soot from the heptane flame. These results highlight the greater sooting propensity of the JP-8 fuel.

Figure 8 shows the variation of the modified extinction coefficient for the JP-8 and heptane pool fires, where the size of the bar corresponds to one standard deviation in the data set about the mean values. These trends are in agreement with results plotted by Murphy and Shaddix in 2006 for JP-8, which are skewed towards the high side of the mean. For heptane, the distribution of the extinction coefficient reveals the opposite trend, which are skewed towards the low side of the mean (Figure 8). These results are consistent with the sooting tendency of the two fuels.

Puffing Frequency

A maximum entropy method (MEM) analysis was carried out at each of the measured heights to identify characteristic frequencies. Results of the MEM analysis

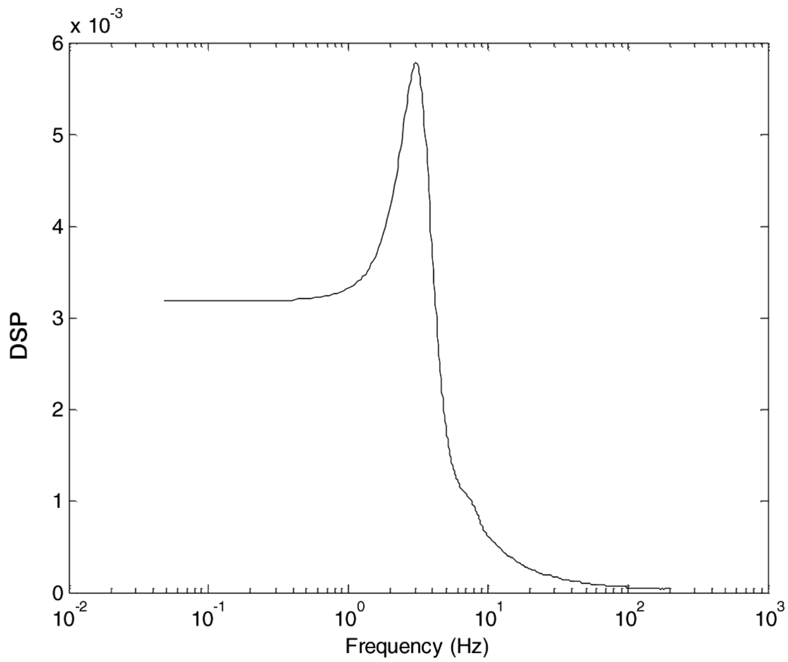

Figure 9 A typical MEM spectra obtained at 435 mm for JP-8.

for both JP-8 and heptane flames clearly identified a single peak for each beam at each height in the flame. An example of one MEM spectra from one beam taken at a height of 435 mm in a JP-8 flame is shown in Figure 9, where a characteristic frequency of approximately 3 Hz is visible. The frequency values obtained from MEM analyses of the extinction data agree well with results for puffing frequency from the literature (Hamins et al., 1992), as shown in Figure 10.

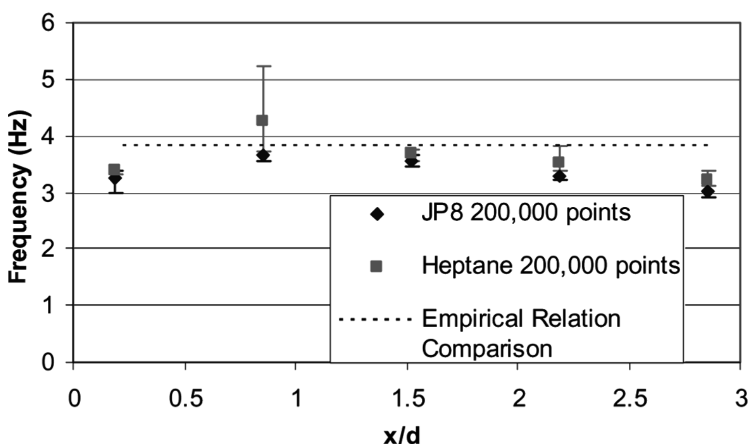

Figure 10 MEM determined extinction frequencies of JP-8 and heptane compared to the corresponding predicted puffing frequencies. Error bars correspond to standard deviation of results for 3 beams at a given height.

The literature value is a constant in this figure since the correlation is only a function of pool diameter. This work illustrates that the measured extinction frequency which corresponds with puffing frequency is a function of height. It is interesting to note that Murphy and Shaddix (2006) found a local relation between soot concentration and puffing frequency, implying that the local soot concentration also exhibits an underlying fluctuation at the same frequency as the puffing of the flame.

Our findings indicate that, since the amount of total soot extinction correlates with the flame's puffing frequency, there is more soot in these large puffs than in the necking region connecting them (Figure 5). This in turn, suggests that the puffs create an environment more suitable for soot formation, such as a longer residence time under fuel rich conditions, or entrainment of more fuel into the puff relative to the neck. There may also be a higher rate of strain in the neck zones between the puffs, which makes the formation of soot more difficult. These results imply that the periods of high extinction correspond to when the beam passes through the puffs, and the periods of low extinction to when the beam passes through the necking region. This interpretation does not necessarily imply a higher local soot volume fraction within the puffs than the neck region – it may simply imply, rather, a longer path length.

The frequency of puffs passing a given height is described by the relation $\mathrm{f_p} = U_{con}/\lambda$, where U_{con} is the convection velocity of the puff and λ is the distance between successive puffs. Hence, a non-constant frequency implies a change in this ratio with height. This could occur, if for example, U_{con} were to change with height, due to buoyant acceleration, assuming λ is constant. Tieszen et al. (2002), showed that, the centre-line fluid velocity first undergoes acceleration and then decelaration during a puffing cycle. Although they did not measure U_{con} directly, it is reasonable to expect that U_{con} will follow a similar trend since, for a cold flow, the convection velocity is proportional to the center line velocity (Hussain and Clark, 1981). Tieszen et al. show that the vertical velocity increases near the bottom of the flame due to the induced radial inflow. An acceleration of the flow combined with necking, is consistent with our measured increase in frequency over the height corresponding to one pool diameter. Higher from the pool surface is a region with reduced vertical velocity due to the radial outflow (Tieszen et al., 2002). This is consistent with our measured decrease in extinction frequency with height above the pool.

In a boundary layer analysis, Puri (1993) assumed the amplitude of the oscillations was a constantly increasing function throughout the flame. Our analysis, shown in Figure 11, reveals that the amplitude of the peaks for JP-8 tends to increase rapidly through the region immediately above the base of the flame. However, upon reaching a height of approximately one pool diameter (intermittent zone), the amplitude of the peaks remains fairly constant thereafter. For heptane, the amplitude of the frequency peaks was found to be approximately constant throughout. The peak amplitudes in the JP-8 flame are greater than in the heptane flame, and this may be due to the presence of unburned soot in and around the region of a puff, rather than in the necking region connecting them, observed for the JP-8 flame only (Figure 5). If the ratio of the amplitude of the extinction to the frequency is taken at each height, a constantly increasing trend for the fluctuations of JP-8 is observed, while these fluctuations remain essentially constant for heptane.

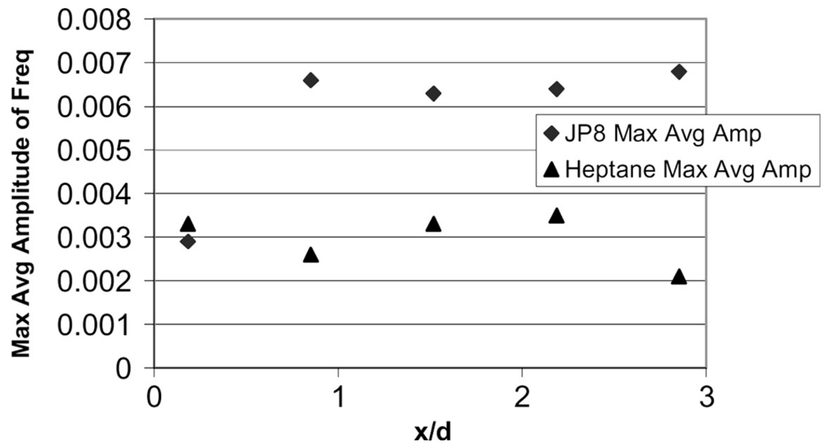

Figure 11 Maximum average amplitude of the frequency peak determined from MEM, calculated over all of the extinguished beams.

Flame Symmetry

The degree of instantaneous axi-symmetry can be assessed by performing correlation statistics on the instantaneous extinction data from the three crossing beams. Correlation coefficients (R) were determined to quantify the instantaneous correlation between beams crossing in the flame according to Eq. (5), where $\bar{x}$ and $\bar{y}$ are the sample means of x_j and y_j, and n is the sample size.

$$R = \frac{\sum_{i=1}^{n}(x_i - \bar{x})(y_i - \bar{y})}{\sqrt{\sum (x_i - \bar{x})^2}\sqrt{\sum (y_i - \bar{y})^2}} \quad -1 \leq R \leq 1 \tag{5}$$

The computed correlation coefficients are plotted in Figure 12.

It should be noted that preliminary calculations of correlation coefficients given by Henriksen et al. (2005) yield a somewhat different trend than those identified in Figure 12. We believe this to be due to the use of too small a sample

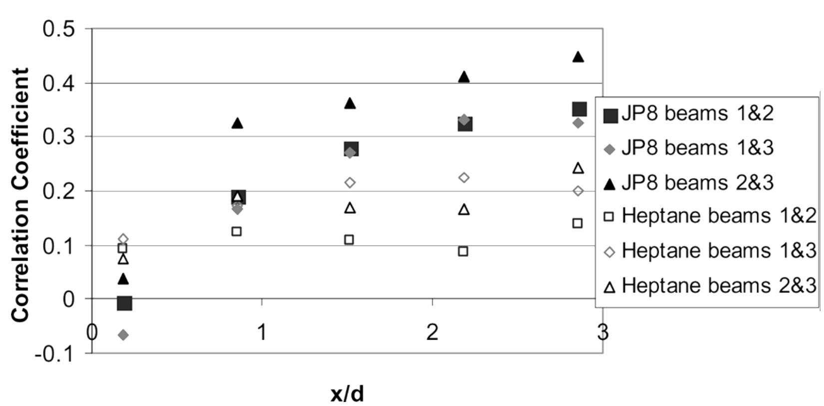

Figure 12 Correlation coefficient between each of the three crossing beams for JP-8 and heptane at each height above the burner surface.

size (4900 points, corresponding to $\sim$4 puffs) for correlation calculations in the earlier study, as compared with the results shown in Figure 12 (200,000 points, $\sim$167 puffs), which represent a much larger portion of the flame's lifetime. Figure 12 clearly demonstrates an increase in axial symmetry of the large scale oscillations for both JP-8 and heptane as height above the pool increases. This is consistent with the puffing motions becoming more dominant with increased height above the pool.

CONCLUSION

A maximum entropy method was used to establish the correlation between total extinction and puffing frequency in JP-8 and heptane pool fires. Small but distinguishable variation in extinction frequency with height was observed for both fuels. The amplitude of this measured frequency was found to be constant at a height greater than one pool diameter. Distribution histograms reveal the spread of the measured data in both fuels, and the standard deviation illustrated the variance in the data set due to turbulence. Finally, correlation statistics revealed an increasing axial symmetry of the large scale oscillations with height relative to the burner axis. Statistical measurements provide experimental evidence of more soot being formed in the puffs than in the necking region connecting them, as well as the presence of quenched soot outside of the flame in the puffing region.

REFERENCES

Becker, H.A. and Yamazaki, S. (1976) Soot concentration field of turbulent propane/air diffusion flames. *Proc. Combust. Instit.*, **16**, 681–691.

Bouhafid, A.,Vantelon, J.P., and Joulain, P. (1988) On the flame structure at the base of a pool fire. *Proc. Combust. Instit.*, **22**, 1291.

Burg, J.P. (1967) Maximum Entropy Spectal Analysis. *37th Meeting of the Society of Exploration Geophysicists*, Oklahoma City, OK.

Eddings, E.G., Yan, S., Ciro, W., and Sarofim, A.F. (2005) Formulation of a surrogate for the simulation of jet pool fires. *Combust. Sci. Technol.*, **177**, 715.

Hamins, A., Yang, J.C., and Kashiwagi, T. (1992). An experimental investigation of the pulsation frequency of flames. *Proc. Combust. Instit.*, **24**, 1695.

Henriksen, T.L., Nathan, G., Alwahabi, Z., Spinti, J., Eddings, E., and Smith, P.J. (2005) Soot volume fraction from extinction in JP-8 and heptane pool fires. *4th Australian Conference on Laser Diagnostics in Fluid Mechanics and Combustion*, Adelaide, South Australia.

Hussain, F. and Clark, A.R. (1981) On the coherent structure of the axisymmetric mixing layer: A flow-visualization study. *J. Fluid Mech.*, **104**, 263–294.

Kohse-Hoinghaus, K. and Jeffries, J.B. (2002) Applied Combustion Diagnostics, 1st ed., Taylor and Francis, New York.

Malalaskera, W.M.G., Versteeg, H.K., and Gilchrist, K. (1996) A review of research and an experimental study on the pulsation of buoyant diffusion flames and pool fires. *Fire Mater.*, **20**, 261.

Murphy, J.J. and Shaddix, C.R. (2006) Soot property measurements in a two-meter diameter JP-8 pool fire. *Combust. Sci Technol.*, **178**, 865.

Puri, I.K. (1993) Prediction of the pulsation frequency of flames formed over a semi-infinite horizontal surface. *Int. J. Heat Mass Trans.*, **36**(10) 2657.

Sato, H., Amagai, K., and Arai, M. (2000) Flickering of diffusion flames observed under various gravity fields. *Proc. Combust. Instit.*, **28**, 1981.

Tieszen, S.R., O'Hern, T.J., Schefer, R.W., Weckman, E.J., and Blanchat, T.K. (2002) Experimental study of the flow field in and around a one meter diameter pool fire. *Combust. Flame*, **129**, 378–391.

Weckman, E.J. and Sobiesiak, A. (1988) The oscillatory behavior of medium scale pool fires. *Proc. Combust. Instit.*, **22**, 1299.

Wu, N. (1997) The Maximum Entropy Method, 1st ed., Springer-Verlag Berlin Heidelberg, New York.

Zukoski, E.E., Cetegen, B.M., and Kubota, T. (1984) Visible structure of buoyant diffusion flames. *Proc. Combust. Instit.*, **20**, 361–366.